October 9, 2013

γ - Z interferometry at a Φ-factory

J. Bernabéu^a, F.J. Botella^{a,b}, O. Vives^a

^{a}Departament de Física Teòrica, Universitat de València and I.F.I.C.
(Centre Mixte Universitat de València–C.S.I.C.)
E-46100 Burjassot (València, Spain)

^{b}Institute for Nuclear Theory, University of Washington
Seattle. WA 98195

Abstract

We analyze the possibilities that the proposed Φ-factories offer to measure $\gamma - Z$ interference. In the unpolarized beam case, we study different signatures in the $\rho\pi$ channel, taking advantage of the presence of the near-by a_1 resonance. We build a C-odd forward-backward asymmetry, estimated to be around 10^{-5}, and (P-even, T-even) and (P-odd, T-odd) alignments of the ρ, to be seen from the angular distribution of its $\pi\pi$ decay products. With polarized electrons a left-right asymmetry around 2×10^{-4} is present in all channels. At leading order this asymmetry is independent of hadronic matrix elements and is sensitive to the $Z^0 - s\bar{s}$ vector coupling. In the $\rho\pi$ channel, a combined left-right forward-backward asymmetry is considered.

arXiv:hep-ph/9512424v2 25 Apr 1996

1 Introduction

A Φ-factory is an e^+e^- collider operating at a center of mass energy $q^2 \simeq (m_\Phi)^2 = (1.01941\,GeV)^2$, so that the dominant process is the formation of the vector resonance $\Phi(1020)$ with spin, parity and charge conjugation $J^{PC} = 1^{--}$. Projected luminosities of $10^{32} - 10^{33}\,cm^{-2}s^{-1}$ at DAΦNE and Novosibirsk [1], would produce more than 10^{10} Φ's per year, a high number that will allow to performe high precision experiments. Different possibilities of testing CP, CPT, chiral lagrangians, etc, can be found in the first and second editions of the DAΦNE Physics Handbook [2].

In this paper we are interested in analyzing the possibilities that a Φ-factory offers to study $\gamma - Z$ interference effects. That is, interference among the γ-dominant contribution to a given final state F (as indicated in Figure 1) and the contribution of the Z-boson (see for example Figure 2).

The interference of Figures 1 and 2 is controlled by the ratio of the Z to γ propagators, so its order of magnitude is $q^2/M_Z^2 \simeq 10^{-4}$. With 10^{10} events per year it seems that this interference could be measured at a Φ-factory like DAΦNE. From this kind of measurement one could isolate the $Z - s\bar{s}$ coupling, in fact the vector coupling (g_V^s), because the Φ is a pure $s\bar{s}$ vector state. Note that the Z also couples to the axial current so there is a contribution coming from the nearest-by axial vector resonance ($J^{PC} = 1^{++}$), the $a_1(1260)$. This resonance has a large width $\Gamma_{a_1} \simeq 400\,MeV$, so at $q^2 \simeq (m_\Phi)^2$ the coupling to the $a_1(1260)$ is still big enough to produce important effects. This interference of Figure 1 with Figures 3 and 4 could give complementary information on the a_1 parameters [3]. In fact the a_1 contribution in Figure 3 is related to $\tau^- \to a_1^- \nu_\tau$ by an isospin rotation.

Other near-by axial vector resonance with a large width is the $h_1(1170)$, a $J^{PC} = 1^{+-}$ state, but the γ and the Z can not couple to this state through the fist-class vector or axial-vector currents because it is a CP odd state. The question of CP violating interferences will be addressed in a forthcoming paper.

Through this paper we will consider only the interference of Figure 1 with the Z-mediated "resonant" contributions of Figures 2, 3 and 4. Non-resonant contributions will be neglected, essentially, because we will only study hadronic final states.

The next point to clarify is where to look for these interference effects. That is, we have to choose the best channels and the best observables to

search for these interferences. First of all we have to keep in mind that the only way to see these effects is to look for distinctive signatures. In a $\gamma - Z$ interference, clearly we only have two signatures of this type. First, the interference of a P-even amplitude with a P-odd one. Second, we can have the interference of a C-odd amplitude with a C-even one. Of course the only kind of signal that unambiguously points towards a $\gamma - Z$ interference is the first one, that is, to look for parity violating observables. Nevertheless we will also study C-odd interferences, but remembering that two photon intermediate states also contribute to these pieces.

The dominant decay channels of the Φ are presented in Table I. Taking into account the number of events necessary to measure an asymmetry of 10^{-4}, we will concentrate in the first three channels. In addition we will distinguish two different cases : we can consider either unpolarized or polarized beams. DAΦNE, for example, is going to operate with unpolarized beams, although electron beam polarization is a possibility that can be considered [4]. So we devote the main part of the paper to study the unpolarized case and at the end we will consider the polarized case, too.

First we analyze the limited possibilities offered by the K^+K^- and K_LK_S channels, and then we will study carefully the more promising $\rho\pi$ channel. We will construct the ρ density matrix and present the observables in the $e^+e^- \rightarrow \rho\pi \rightarrow \pi\pi\pi$ channels. Again both channels will be analyzed in the polarized beam case.

2 $e^-e^+ \rightarrow K^+K^-, K_S K_L$

The a_1 does not couple to $K\bar{K}$ strongly because of Parity. So in this channel we only have the interference of Figure 1 with Figure 2. The relevant piece would be when the Z couples to e^-e^+ through the axial current, so we need to construct a pseudoscalar quantity. But kaons have no spin, and with unpolarized beams we don't have any pseudoscalar to our disposal in this process.

In conclusion the dominant channels are not useful to measure the $\gamma - Z$ interference in the case of unpolarized beams. As we will see later, the situation changes in the case of polarized beams.

3 $e^- e^+ \rightarrow \rho\pi$

In this channel we have a particle with spin in the final state and both Φ and a_1 couple to $\rho\pi$. So the arguments given in the previous section go into the opposite direction, that is, we can expect this channel to be the one where a $\gamma - Z$ interference signal at a Φ-factory with unpolarized beams can be expected.

3.1 ρ-density matrix $\rho^{\mathbf{out}}$

In the process $e^-(l_-, \lambda_-) + e^+(l_+, \lambda_+) \rightarrow \rho(k, \sigma) + \pi(p)$ for unpolarized initial $e^- e^+$ all the observables are in the ρ-density matrix ρ^{out}, because the pion has no spin.

In the center of mass frame (C.M.), in the so-called helicity convention [5], for an electron with momentum l_- and helicity λ_- and a positron with momentum l_+ and helicity λ_+, the amplitude to a π with momentum p, and a ρ with momentum k and helicity σ is given by [5]

$$f_{\sigma,\vec{\lambda}}(\theta, \phi) = N \, exp(i\lambda\phi) \sum_J (2J + 1) \, d^J_{\lambda,\sigma}(\theta) \, T^J_{\sigma,\vec{\lambda}} \tag{1}$$

where $\vec{\lambda} = (\lambda_-, \lambda_+)$, $\lambda = \lambda_- - \lambda_+$, (θ, ϕ) are defined in Figure 5, $d^J_{\lambda,\sigma}(\theta)$ are the reduced rotation matrices about the y-axis, and the $T^J_{\sigma,\vec{\lambda}}$ are the so-called reduced helicity amplitudes. In our case, because in all diagrams $e^+ e^-$ couple to a vector boson, the sum in Equation (1) gets reduced to the term $J = 1$. So we can write Equation (1) in a more simple way

$$f_{\sigma,\vec{\lambda}}(\theta, \phi) = d^1_{\lambda,\sigma}(\theta) \, T_{\sigma,\lambda} \tag{2}$$

To write Equation (2), we have chosen the scattering plane as the x-z plane defined in Figure 5. We have defined $3NT^1_{\sigma,\vec{\lambda}} = T_{\sigma,\lambda}$. Finally we have performed the approximation of neglecting the electron mass; in this case, the vector and axial vector currents conserve helicity at the electron vertex. So the only amplitudes we can have are the ones with $\vec{\lambda} = (+\frac{1}{2}, -\frac{1}{2})$ or $\vec{\lambda} = (-\frac{1}{2}, +\frac{1}{2})$, that means that λ can take the values $\lambda = \lambda_- - \lambda_+ = \pm 1$ and λ fixes $\vec{\lambda}$.

In Appendix A we give the ρ^{out} density matrix in general for processes dominated by vector boson contributions, that is, for the amplitudes given

by Equation (2). If we consider the contribution of the diagrams in Figures 1 to 4 we can write .

$$T_{\sigma,\lambda} = T_{\sigma,\lambda}(\Phi_\gamma) + T_{\sigma,\lambda}(\Phi_Z) + T_{\sigma,\lambda}(a_1^V) + T_{\sigma,\lambda}(a_1^A) + T_{\sigma,\lambda}(\Phi - a_1) \quad (3)$$

where $T_{\sigma,\lambda}(\Phi_\gamma)$ is the contribution of Figure 1, $T_{\sigma,\lambda}(\Phi_Z)$ is the parity violating piece in Figure 2, the parity conserving piece in Figure 2 will not be considered, because essentially it has the same structure than Figure 1. $T_{\sigma,\lambda}(a_1^A)$ and $T_{\sigma,\lambda}(a_1^V)$ are respectively the P-conserving and P-violating pieces of Figure 3. Finally $T_{\sigma,\lambda}(\Phi - a_1)$ is the contribution of Figure 4, that violates parity.

Now it is evident that $T_{\sigma,\lambda}(\Phi_\gamma)$ and $T_{\sigma,\lambda}(a_1^A)$ are P even and $T_{\sigma,\lambda}(a_1^V)$, $T_{\sigma,\lambda}(\Phi_Z)$ and $T_{\sigma,\lambda}(\Phi - a_1)$ are P odd so they verify [5]

$$\begin{aligned}
T_{\sigma,\lambda}(\Phi_\gamma, a_1^A) &= -T_{-\sigma,-\lambda}(\Phi_\gamma, a_1^A) \\
T_{\sigma,\lambda}(\Phi_Z, a_1^V, \Phi - a_1) &= +T_{-\sigma,-\lambda}(\Phi_Z, a_1^V, \Phi - a_1)
\end{aligned} \quad (4)$$

Also from parity conservation in $\Phi \to \rho\pi$ and $a_1 \to \rho\pi$ decays we have

$$\begin{aligned}
T_{\sigma,\lambda}(\Phi_\gamma, \Phi_Z) &= -T_{-\sigma,\lambda}(\Phi_\gamma, \Phi_Z) \\
T_{\sigma,\lambda}(a_1^A, a_1^V, \Phi - a_1) &= +T_{-\sigma,\lambda}(a_1^A, a_1^V, \Phi - a_1)
\end{aligned} \quad (5)$$

Note that a Φ can not decay to a ρ with helicity $\sigma = 0$. From Equations (4) and (5) it is possible to write all the reduced helicity amplitudes in terms of the following pieces : $T_{1,1}(\Phi_\gamma)$, $T_{1,1}(\Phi_Z)$, $T_{1,1}(a_1^A)$, $T_{1,1}(a_1^V)$, $T_{1,1}(\Phi - a_1)$, $T_{0,1}(a_1^A)$, $T_{0,1}(a_1^V)$ and $T_{0,1}(\Phi - a_1)$. Here the most important piece is the first one, being the other seven of order 10^{-4} with respect to the first one, at least.

Using the equations in Appendix A we get for the cross section

$$\sigma = \int (\frac{d\sigma}{d\Omega}) d\Omega = \frac{16\pi}{3} |T_{1,1}(\Phi_\gamma)|^2 \quad (6)$$

$$\frac{d\sigma}{d\Omega} = Tr(\rho^{out}) = \frac{3\sigma}{16\pi} \{(1 + \cos^2\theta) + 4Re[\frac{T_{1,1}(a_1^A)}{T_{1,1}(\Phi_\gamma)}]\cos\theta\} \quad (7)$$

4

with θ the polar angle of the ρ with respect to the electron beam.

In Equation (6) we give the integrated cross section. In fact this equation fixes the normalization of the reduced helicity amplitudes. Equations (6) and (7) are valid under the assumption of using the electromagnetic amplitude squared and the γ-Z interference. As we can see in Equation (7), it appears for the first time a $\gamma - Z$ interference. The second term in the right hand side (r.h.s.) of Equation (7) gives a forward-backward asymmetry as one would expect from an interference of the vector×vector (V-V) piece in diagram 1 with the axial×axial (A-A) piece in diagram 3. It must be stressed at this time that, in general, any interference of the type (V-V)(A-A) can also be produced by interference of diagram 1 with two photon processes. Note that the 2γ contribution is P-even and C-even as the (A-A) piece in Figure 3. Two photons in the intermediate state can not couple to any $0^{\pm}$ resonance because of helicity supresion. Landau-Yang theorem [6] forbids the coupling of two real photons to $1^{\pm}$ states, so it remains the resonant contribution $e^+e^- \to \gamma\,\gamma^* \to a_1^0 \to ...$, where the virtual photon γ^* is coupled to ρ^0 or ω.

From reference [7], we can obtain a rigurous lower bound for this contribution provided the amplitudes $a_1^0 \to \rho^0\gamma$, $a_1^0 \to \omega\gamma$, $\rho^0 \to \gamma$ and $\omega \to \gamma$ are known. These can be borrowed from the spin-1 chiral Lagrangian of ref. [8] based on an extended Nambu-Jona-Lasinio model of QCD. With these inputs we get for the ratio of the absorptive part of the $\gamma(\rho^0,\omega)$ amplitude to the weak amplitude :

$$\frac{|A(a_1 \to e^+e^-)_{\gamma\gamma^*}|}{|A(a_1 \to e^+e^-)_{weak}|} \geq 8.5 \tag{8}$$

Although this result indicates that the natural order of magnitude of the $\gamma\,\gamma^*$ contribution to the forward-backward asymmetry is larger than the weak one, it must be stressed that there is also the contribution of the $\gamma\,\gamma^*$ dispersive part. The forward-backward asymmetry comes from an interference, so one can get some cancellation or enhancement between the absorptive and dispersive $\gamma\,\gamma^*$ pieces. Thus no definite conclusion about electromagnetic or weak dominance can be extracted from equation (8) till a complete analysis of the process $e^+e^- \to \gamma\,\gamma^* \to a_1$ has been done [9].

The next set of observables that can be measured in this channel correspond to the alignments of the ρ, that is, the second-rank multipolar parameters $t_{2,M}$, defined in Appendix A. For these observables we get

5

$$\frac{d\sigma}{d\Omega} t_{2,0}(\theta) = \sqrt{\frac{1}{10}} \frac{d\sigma}{d\Omega} \tag{9}$$

$$\frac{d\sigma}{d\Omega} t_{2,1}(\theta) = \sqrt{\frac{3}{5}} \sin\theta \{Re[T_{0,1}(a_1^A)T_{1,1}^*(\Phi_\gamma)]$$
$$+ i\cos\theta Im[(T_{0,1}(a_1^V) + T_{0,1}(\Phi - a_1)) T_{1,1}^*(\Phi_\gamma)]\} \tag{10}$$

$$\frac{d\sigma}{d\Omega} t_{2,2}(\theta) = \sqrt{\frac{3}{5}} \frac{\sin^2\theta}{2} \{-|T_{1,1}(\Phi_\gamma)|^2$$
$$+ 2iIm[(T_{1,1}(a_1^V) + T_{1,1}(\Phi - a_1)) T_{1,1}^*(\Phi_\gamma)]\} \tag{11}$$

From Equations (10) and (11) we can see that the imaginary parts of $t_{2,1}$ and $t_{2,2}$ contain parity violating pieces of the type (V-V)(V-A), both from Figures 3 and 4, so these terms unambiguously point to a $\gamma - Z$ interference. It must be stressed that the amplitudes that interfere in these observables must be not relatively real, this points out to T odd observables as we will see. Note that Figure 2 does not contribute to these Parity violating pieces , so the Z-$s\bar{s}$ coupling will appear only from the diagram of Figure 4, where there is a contribution proportional to g_V^s. In Equation (10) we have an additional P conserving $\gamma - Z$ interference that can get contribution also from diagrams with two photons.

For completeness we also give the first-rank multipolar parameters $t_{1,M}(\theta)$, but in a more standard notation of polarization components. The angular distributions of the polarization along the x', y' and z' axes defined in Figure 5 are given by

$$\frac{d\sigma}{d\Omega} P_{x'}(\theta) = -2Re[(T_{0,1}(a_1^V) + T_{0,1}(\Phi - a_1)) T_{1,1}^*(\Phi_\gamma)] \sin\theta \cos\theta \tag{12}$$

$$\frac{d\sigma}{d\Omega} P_{y'}(\theta) = -2Im[T_{0,1}(a_1^A)T_{1,1}^*(\Phi_\gamma)] \sin\theta \tag{13}$$

$$\frac{d\sigma}{d\Omega} P_{z'}(\theta) = 2Re[(T_{1,1}(a_1^V) + T_{1,1}(\Phi - a_1))T_{1,1}^*(\Phi_\gamma)] (1 + \cos^2\theta)$$
$$+ 4Re[T_{1,1}(\Phi_Z)T_{1,1}^*(\Phi_\gamma)] \cos\theta \tag{14}$$

As is well-known, the only parity-violating polarizations are within the scattering plane, and correspond to $P_{x'}$ and $P_{z'}$. $P_{y'}$, being a T odd observable, needs a relative phase among interfering amplitudes. It has to be pointed out that these polarization interferences are rather difficult to measure. Looking at the $\rho \to \pi\pi$ channel is useless, because the pions have no spin, and ρ decays through a parity conserving interaction. The ρ^+ decay channels are badly measured so we do not know if there is some channel with branching ratio at the level of 10^{-3} that can be used to measure the ρ-polarization. In any case if there is such a channel, even a polarization at the 10^{-3} level is going to be difficult to measure. So we will not consider ρ-polarization as being a measurable quantity at a Φ-factory, at least at the required level of accuracy to see γ-Z interference in the $\rho^\pm\pi^\mp$ channels.

In order to measure the ρ^0 polarization, there is a channel that probably could be used: $\rho^0 \to \pi^+\pi^-\gamma$ whose branching ratio is of order 10^{-2}. In any case sensitivities to the level of 10^{-4} seem difficult to obtain. It must be stressed that there is only the second piece in the r.h.s. of Equation (14) that can contribute to polarize the ρ^0, $a_1 \to \rho^0\pi^0$ is forbidden by C, therefore only the interference with Figure 2 can contribute to the $\rho^0\pi^0$ channel. Being this piece sensitive to the $Z - s\bar{s}$ vector coupling (g_V^s), it would be interesting to analyze the sensitivity to g_V^s of a triple correlation in the process $e^+e^- \to$ "Φ" $\to \rho^0\pi^0 \to (\pi^+\pi^-\gamma)\pi^0$ [9].

Except for this last comment, we must conclude that although there are several pieces sensitive to the $\gamma - Z$ interference in our observables, it looks hard if not impossible to measure the contribution of g_V^s coming from Figure 2 with unpolarized beams.

3.2 The ρ-density matrix ρ^{out} and the $Z - s\bar{s}$ coupling

Let us try to understand Equations (9) to (14) in a simple way. Equations (12), (13) and (14) are proportional to $\langle \vec{s}\cdot(\alpha\vec{k}+\beta\vec{l_-})\rangle \approx \langle S_{x'}\rangle$, $\langle \vec{s}\cdot(\vec{k}\times\vec{l_-})\rangle \approx \langle S_{y'}\rangle$ and $\langle \vec{s}\cdot\vec{k}\rangle \approx \langle S_{z'}\rangle$ respectively, so clearly $S_{x'}$ and $S_{z'}$ are P-odd and T-even, consequently they are proportional to the "real" part of a parity-violating interference. On the contrary $S_{y'}$ is P-even and T-odd and then it is proportional to the "imaginary" part of a parity-conserving interference. Note also that $S_{x'}$ and $S_{y'}$ are a combination of the $S_\pm$ operators, so they need two different amplitudes that differ by one unit in the helicity of the

<center>7</center>

ρ. However Figure 2 does not populate the ρ in the helicity state $\sigma = 0$, so it can only contribute to $P_{z'}$. The other results follow inmediatelly from the previous arguments.

If we take into account the following relations for the spherical components of the tensor polarization

$$
\begin{aligned}
T_{2,0} &\propto (3S_{z'}^2 - \vec{S}^2) && (15) \\
T_{2,1} &\propto (S_+ S_{z'} + S_{z'} S_+) \propto (S_{x'} S_{z'} + S_{z'} S_{x'}) + i(S_{y'} S_{z'} + S_{z'} S_{y'}) \\
T_{2,2} &\propto S_+^2 \propto S_{x'}^2 - S_{y'}^2 + i(S_{y'} S_{x'} + S_{x'} S_{y'})
\end{aligned}
$$

it is quite easy to understand the result in Equations (9), (10) and (11). $\langle T_{2,0} \rangle$, being proportional to S_i^2, must be P-even and T-even, thus the forward-backward asymmetry is proportional to the "real" part of a P-conserving interference. $\langle T_{2,1} \rangle$ has two pieces, the real part proportional to $\langle (S_{x'} S_{z'} + S_{z'} S_{x'}) \rangle$ must be P-even and T-even, and so proportional to the "real" part of a P-conserving interference, as it is. The imaginary part of $\langle T_{2,1} \rangle$ is proportional to $\langle (S_{y'} S_{z'} + S_{z'} S_{y'}) \rangle$, and so it is P-odd and T-odd, consequently it gives the "imaginary" part of a parity-violating interference. The reason why Figure 2 does not contribute to $T_{2,1}$ is again the absence of population in the $\sigma = 0$ helicity state of the ρ. Being $T_{2,1}$ linear with $S_{y'}$ the contributions to $\langle T_{2,1} \rangle$ are proportional to the interference of two amplitudes differing by one unit in the ρ -helicity. On the contrary Figure 4 is proportional to g_V^s and it contributes to this P-violating piece.

Finally from the last of Eqs. (15), the imaginary part of $\langle T_{2,2} \rangle$ is itself the imaginary part of a P-violating interference, because $S_{x'} S_{y'}$ is P-odd and T-odd. Why Figure 2 does not contribute to this piece ?. If we study only contributions from Figure 1 and 2, our process can be studied as a two step process : first the formation of a polarized and aligned Φ, polarized by the interference of Figures 1 and 2, and aligned (just $t_{2,0}$) by Figure 1 alone, followed by its decay $A \rightarrow B(J = 1) + C$, it can be checked than in order to obtain $t_{2,2} \neq 0$ for the B-particle (of spin 1) , it is necessary to have the A-particle aligned. This is why Figure 1 contributes to the real part of $t_{2,2}$ (P-even and T-even) and why Figure 2 does not contribute to the imaginary part of $t_{2,2}$ (P-odd and T-odd); Figure 2 does not aligne the Φ and consequently does not contribute to $t_{2,2}$. Note that in this argument we have not used the fact that $T_{\sigma,\lambda}(\Phi_\gamma)$ and $T_{\sigma,\lambda}(\Phi_Z)$ have the same relative phases,

that also implies $Im(t_{2,2}) = 0$ from Figure 2. Once again this argument does not apply to Figure 4, which also contributes to Eq. (15).

In conclusion, we understand why g_V^s coming from Figure 2 appears only in the second piece of $P_{z'}(\theta)$. Therefore, with unpolarized beams it seems difficult to extract g_V^s from the contribution of Figure 2 with Φ-factory data, although there is still the contribution of Figure 4, proportional to g_V^s too.

4   Observables in $e^- e^+ \rightarrow \rho^+ \pi^- \rightarrow (\pi^+ \pi^0) \pi^-$

To measure the multipolar parameters of ρ, one has to look at the correlated decay of the ρ. To be specific we will consider the channel $\rho^+ \pi^-$ and the subsequent decay $\rho^+ \rightarrow \pi^+ \pi^0$, that for our purpose has 100% branching ratio. The amplitude for a ρ^+ with third component of spin σ to decay to $\pi^+ \pi^0$ (π^+ in the direction Ω_1) in its center of mass frame is given by

$$f_\sigma(\Omega_1) = (\frac{3}{4\pi})^{\frac{1}{2}} \mathcal{D}_{\sigma,0}^{(1)}(\phi_1, \theta_1, 0) T \tag{16}$$

The single important factor here is the rotation matrix $\mathcal{D}_{\sigma,0}^{(1)}(\phi_1, \theta_1, 0)$. Ω_1 is the direction of the π^+ in the C.M. of the ρ, with respect to the axes we have defined in Figure 5 (x',y',z'). T is the unique reduced helicity amplitude present here, so it will be controlled by the width $\Gamma(\rho^+ \rightarrow \pi^+ \pi^0) = |T|^2$. Having this channel 100% branching ratio, we can take $|T|^2$ equal to the total width of the ρ, and so we get

$$\frac{d^2\sigma}{d\Omega d\Omega_1} = \frac{1}{|T|^2} \sum_{\sigma,\sigma'} f_\sigma(\Omega_1) \rho_{\sigma,\sigma'}^{out}(\Omega) f_{\sigma'}^*(\Omega_1) \tag{17}$$

This expresion represents the differential cross section for $e^+ e^- \rightarrow \rho^+ \pi^-$ and the subsequent decay $\rho^+ \rightarrow \pi^+ \pi^0$ in the $e^+ e^-$ C.M. frame and expressed in terms of $\Omega = (\theta, \phi)$ and $\Omega_1 = (\theta_1, \phi_1)$, the angle of the π^+ in the ρ^+ C.M.. The result of Eq. (17) is independent of the dynamics (T) of ρ decay. Note that $\rho_{\sigma,\sigma'}^{out}$ is invariant under a boost along the direction of motion of the ρ. It is now straight-forward to get

$$\frac{d^2\sigma}{d\Omega d\Omega_1} = \frac{d\sigma}{d\Omega}(e^+ e^- \rightarrow \rho^+ \pi^-) \frac{1}{4\pi} [1 - \sqrt{10} \sum_N \mathcal{D}_{N,0}^{(2)}(\phi_1, \theta_1, 0) t_{2,N}(\theta)] \tag{18}$$

9

As we have previously discussed, the multipolar parameters $t_{1,M}$ (the usual polarizations) have disappeared from the final angular distribution, and only the second-rank multipolar parameters can be measured. So our final expresion for the $\rho^+\pi^-$ channel is

$$\frac{d^2\sigma}{d\Omega d\Omega_1} = \frac{9\sigma(e^+e^- \to \rho^+\pi^-)}{128\pi^2}\{[(1 + \cos^2\theta) + 4Re[\frac{T_{1,1}(a_1^A)}{T_{1,1}(\Phi_\gamma)}]\cos\theta]\sin^2\theta_1$$
$$+ [Re[\frac{T_{0,1}(a_1^A)}{T_{1,1}(\Phi_\gamma)}]\cos\phi_1 + Im[\frac{T_{0,1}(a_1^V) + T_{0,1}(\Phi - a_1)}{T_{1,1}(\Phi_\gamma)}]\cos\theta\sin\phi_1]4\sin\theta\sin\theta_1$$
$$\cos\theta_1 + [\cos(2\phi_1) - 2Im[\frac{T_{1,1}(a_1^V) + T_{1,1}(\Phi - a_1)}{T_{1,1}(\Phi_\gamma)}]\sin(2\phi_1)]\sin^2\theta\sin^2\theta_1\} \tag{19}$$

As can be seen from this expresion, the $\gamma - Z$ interference has produced four new asymmetries, one of them also present at the $\rho^+\pi^-$ level. Two of them violate parity and the other two are parity conserving. These asymmetries can be extracted by fitting the real data with Equation (19) or by measuring the following observables

$$\langle\cos\theta\rangle = Re[\frac{T_{1,1}(a_1^A)}{T_{1,1}(\Phi_\gamma)}] \tag{20}$$

$$\langle\cos\theta_1\cos\phi_1\rangle = (\frac{3\pi}{16})^2 Re[\frac{T_{0,1}(a_1^A)}{T_{1,1}(\Phi_\gamma)}] \tag{21}$$

$$\langle\cos\theta\cos\theta_1\sin\phi_1\rangle = \frac{1}{4}(\frac{3\pi}{16})^2 Im[\frac{T_{0,1}(a_1^V) + T_{0,1}(\Phi - a_1)}{T_{1,1}(\Phi_\gamma)}] \tag{22}$$

$$\langle\sin 2\phi_1\rangle = -\frac{1}{2}Im[\frac{T_{1,1}(a_1^V) + T_{1,1}(\Phi - a_1)}{T_{1,1}(\Phi_\gamma)}] \tag{23}$$

From (B.4) we see that the Φ coupling does not change when going from the $\rho^+\pi^-$ to the $\rho^-\pi^+$ channel, but from (B.12) the a_1 coupling changes sign from $\rho^+\pi^-$ to $\rho^-\pi^+$. So Equation (19) will also be valid for the $\rho^-\pi^+$ channel, except that all the asymmetries will change sign. From (B.11) we know that the a_1 does not couple to $\rho^0\pi^0$, so in this channel these four asymmetries vanish. Although we have derived these results from Isospin, actually

they can also be obtained from C invariance of strong and electromagnetic interactions, and so this result is more general. It must be pointed out that, by comparing different charge channels, one can eliminate some systematic errors, for example, by performing the ratio of the difference over the sum of the $\rho^+\pi^-$ and $\rho^-\pi^+$ channels.

Equation (19) has been obtained under the assumption of the narrow width aproximation for the ρ, this means that the imaginary parts of equations (22) and (23) comes from the relative phase among the Φ and a_1 propagators at the Φ peak. If the finite width of the ρ is taken into account, three intermediate resonant ρ's have to be included in Figures 1 and 2, and ρ^+ and ρ^- in Figures 3 and 4. This fact will bring more phases into the game in such a way that the results in equations (22) and (23) will change. These complications will be considered numerically in the next section. Nevertheless, we must stress that the inclusion of these additional interferences does not change the argument in section 3.3 about the absence of any contribution of Figure 2 to the observable (23). In fact, the parity violating piece of Figures 1 and 2 with three pions in the final state is proportional to an antisymmetric leptonic tensor contracted with a "symmetric" hadronic tensor, thus this contribution vanishes. Note that there is only one form factor for the matrix element of the vector current between three pions and the vacuum, so in the three pion channel this interference is never present, even if we include finite widths and interference of three intermediate ρ's.

5   Numerical results: unpolarized beams

Now we will present our estimate of the four asymmetries appearing in Equation (19). Let us for example concentrate in the one that gives a forward-backward asymmetry at the $\rho^+\pi^-$ level.

$$A_{FB} = \frac{\sigma(\cos\theta > 0) - \sigma(\cos\theta < 0)}{\sigma(\cos\theta > 0) + \sigma(\cos\theta < 0)} = \frac{3}{2}\langle\cos\theta\rangle = \frac{3}{2}Re[\frac{T_{1,1}(a_1^A)}{T_{1,1}(\Phi)}] \qquad (24)$$

From Equation (C.12) and (C.17) we get

$$A_{FB} = -\frac{9}{2\sqrt{2}}\left(\frac{G_F q^2}{4\pi\alpha}\right)\frac{|\vec{k}|}{k^0}\frac{|F_A(q^2)||A_1(q^2)|}{|F_V(q^2)||\Phi(q^2)|}Re[e^{iw_1}\frac{P_{a_1}(q^2)}{P_\Phi(q^2)}] \qquad (25)$$

where we have substituted the couplings of the standard model, and also we have introduced a potential relative phase among $F_A A_1$ and $F_V \Phi$, more likely $w = 0$ or π. Now we need values for all the form factors appearing in (25).

From the width $\Phi \to e^+ e^-$ [3], Equation (B.2), we get

$$|F_V(M_\Phi^2)| = 0.242 \, GeV^2 \tag{26}$$

From $\tau \to \nu_\tau a_1$, that can be roughly extracted from the three pion channel [10], we get using (B.9)

$$|F_A(q^2 \simeq M_{a_1}^2)| = 0.198 \, GeV^2 \tag{27}$$

This result is also in agreement with a recent lattice calculation [11], taking into account an $\sqrt{2}$ factor of difference in the normalization. From $\Phi \to \rho^+ \pi^-$ [3] and Equation (B.5) we get

$$|\Phi(M_\Phi^2)| = 1.10 \, GeV^{-1} \tag{28}$$

Finally, assuming that a_1 decays dominantly [3] to $\rho\pi$ and taking a width of $400 \, MeV$ we get

$$|A_0(q^2 \simeq M_{a_1}^2)| \leq 39.5 \, GeV^{-1} \tag{29}$$

$$|A_1(q^2 \simeq M_{a_1}^2)| \leq 30.8 \, GeV^{-1} \tag{30}$$

In principle, there is no apparent dynamical reason why A_0 should be much bigger than A_1 or viceversa. Just for illustrative purpose, we can quote than in the model of reference [12] the ratio A_0/A_1 gets the value -1.19. In this particular model, Equation (B.13) and $\Gamma_{a_1} = 400 \, MeV$ translate into the following values: $|A_0| \simeq 26.9 \, GeV^{-1}$ and $|A_1| \simeq 22.6 \, GeV^{-1}$. ARGUS collaboration has also measured the A_0/A_1 ratio (S/D ratio) [13] and these results agree, within errors, with the calculation of reference [12]. Then, to estimate the asymmetries we will use these values from ARGUS measurements, but keeping in mind that the results may slightly differ from our estimates, because the data are not good enough in the Φ region. In fact, if only the limits given by Eqs. (29) and (30) were considered, all observables could reach values 1.4 higher than our estimated results.

So just using experimental values and assuming no q^2-dependence for the $|A_1(q^2)|$ form factor we get

$$|A_{FB}(q^2 \simeq M_{a_1}^2)| \simeq 1.63 \times 10^{-3} |Re[e^{iw_1} \frac{P_{a_1}(q^2)}{P_\Phi(q^2)}]| \qquad (31)$$

A Φ-factory is going to operate essentially at the Φ-peak, also the Φ Breit-Wigner structure can not be extrapolated from the Φ-peak more than a few times the Φ width Γ_Φ, so we define the variable ϵ as $q^2 = (M_\Phi + \epsilon\Gamma_\Phi)^2$ and we will consider only the range $-2 \leq \epsilon \leq 2$ for illustrations.

For pure Breit-Wigner structures as in (C.6) we get

$$\frac{P_{a_1}(q^2)}{P_\Phi(q^2)} = \frac{M_\Phi \Gamma_\Phi}{M_{a_1} \Gamma_{a_1}} \, G(\epsilon) \qquad (32)$$

where $G(\epsilon)$ is the function

$$G(\epsilon) = \{\frac{1 + g(\epsilon)f(\epsilon)}{1 + f^2(\epsilon)} + i\frac{f(\epsilon) - g(\epsilon)}{1 + f^2(\epsilon)}\} \qquad (33)$$

and the f and g functions are defined as follows

$$g(\epsilon) = 2\epsilon(1 + \frac{\epsilon\Gamma_\Phi}{2M_\Phi}) \qquad (34)$$

$$f(\epsilon) = -x + \frac{M_\Phi \Gamma_\Phi}{M_{a_1} \Gamma_{a_1}} g(\epsilon) \qquad (35)$$

$x = (M_{a_1}^2 - M_\Phi^2)/(M_{a_1}\Gamma_{a_1})$. For $\Gamma_{a_1} = 400\,MeV$ x gets the value 0.98. The real part of Equation (32) vanishes for $\epsilon \simeq 1/(2x)$ and the imaginary one equals to zero at $\epsilon \simeq -x/2$. These cancellations make difficult to give any precise value for A_{FB}, taking into account: the uncertainties in Γ_{a_1}, the poor approximation that represents the pure Breit-Wigner structure for the a_1 and the lack of knowledge of w_1. Up to unfortunate cancellations, it is the factor $(M_\Phi\Gamma_\Phi)/(M_{a_1}\Gamma_{a_1}) \simeq 9.18 \times 10^{-3}$ that sets the scale in Equation (32).

So a reasonable estimate of Equation (31) would be to take $\epsilon = 0$ and $w_1 = 0$. In that case we get, always for $\Gamma_{a_1} = 400\,MeV$

$$|A_{FB}(q^2 \simeq M_{a_1}^2)|_{w_1=0} \simeq 7.76 \times 10^{-6} \qquad (36)$$

In Figure 6 we have plotted $G(\epsilon)$ for $\Gamma_{a_1} = 400MeV$, and, as far as orders of magnitude are concerned, it can be seen that both the real and the imaginary parts of $G(\epsilon)$ are similar.

13

Comparing Equations (C.17) and (C.16), it is evident that, up to minor kinematical changes, $Re[\frac{T_{0,1}(a_1^A)}{T_{1,1}(\Phi_\gamma)}]$ is equal to $\langle\cos\theta\rangle$ except for the change A_1 by A_0, so we get in the same spirit than Equation (36)

$$|Re[\frac{T_{0,1}(a_1^A)}{T_{1,1}(\Phi_\gamma)}]|_{w_1=0} \simeq 6.31 \times 10^{-6} \tag{37}$$

Using (C.5), (C.14) and (C.15), we can give the parity violating asymmetries in Equations (22) and (23), for $sin^2\theta_W = 0.23$

$$|Im[\frac{T_{0,1}(a_1^V) + T_{0,1}(\Phi - a_1)}{T_{1,1}(\Phi_\gamma)}]|_{w_1=0} \simeq$$
$$5.27 \times 10^{-3}|Im[(g_V - i\frac{9\eta g_V^s}{\alpha}B.r.(\Phi \to e^+e^-))\frac{P_{a_1}}{P_\Phi}]| =$$
$$5.27 \times 10^{-3}|g_V Im[\frac{P_{a_1}}{P_\Phi}] - 0.38\eta g_V^s Re[\frac{P_{a_1}}{P_\Phi}]| =$$
$$(4.85 \times 10^{-2} + 1.44|g_V^s|)10^{-5} \simeq 2.98 \times 10^{-6} \tag{38}$$

$$|Im[\frac{T_{1,1}(a_1^V) + T_{1,1}(\Phi - a_1)}{T_{1,1}(\Phi_\gamma)}]|_{w_1=0} \simeq (3.96\times10^{-2}+1.17|g_V^s|)10^{-5} \simeq 2.42\times10^{-6} \tag{39}$$

As we can see, the dominant piece comes from Figure 4, and so it is proportional to g_V^s. Nevertheless these asymmetries are difficult to be measured at a Φ-factory. For the observables (22) and (23) these results translate into

$$\langle\cos\theta\cos\theta_1\sin\phi_1\rangle = 2.58 \times 10^{-7} \tag{40}$$

$$\langle\sin 2\phi_1\rangle = 1.21 \times 10^{-6} \tag{41}$$

If finite width effects are included ($\Gamma_\rho = 150MeV$) by introducing three intermediate ρ's in Figure 1 and ρ^+ and ρ^- in Figures 3 and 4 the results change a little bit. These observables have to be integrated over some region of the invariant mass of the $\pi^+\pi^-$ system. If we take this region to be $[(m_\rho - \Gamma_\rho)^2, (m_\rho + \Gamma_\rho)^2]$, inside the phase space and a pure Breit-Wigner structure for the ρ-propagator we get

$$\langle \cos\theta \cos\theta_1 \sin\phi_1 \rangle = 1.21 \times 10^{-7} \tag{42}$$

$$\langle \sin 2\phi_1 \rangle = 1.35 \times 10^{-6} \tag{43}$$

As can be seen from these results, the narrow width approximation is quite good for $\langle \sin 2\phi_1 \rangle$, but for $\langle \cos\theta \cos\theta_1 \sin\phi_1 \rangle$ the corrections due to the finite (and large) width of the ρ become important.

6   Polarized beams : Left-Right asymmetries

As previously mentioned, at a Φ-factory like DAΦNE , in principle it would be possible to operate the machine with polarized electrons without a serious drawback in its luminosity [4]. So we will consider in this section the case when electrons are longitudinally polarized, with polarization P, and positrons are unpolarized. In this situation it is easy to construct a pseudoscalar quantity, as is the case for the so-called left-right asymmetry

$$A_{LR} = \frac{\sigma(P) - \sigma(-P)}{\sigma(P) + \sigma(-P)} \tag{44}$$

where $\sigma(P)$ is the integrated cross section for a given channel F when the initial electron is longitudinally polarized with value P. This asymmetry will arise from the interference of the diagrams in Figure 1 and 2, for any decay channel.

Note that if we integrate over the F variables, the hadronic tensor is symmetric and the symmetric part of the leptonic tensor is the same both for the leading term coming from the Figure 1 - P independent - and the interference with Figure 2 - this piece being proportional to P - . Other diagrams do not contribute at leading order to this observable. Taking this fact into account, we can write $\sigma(P)$ as

$$\sigma(P) = \sigma(P=0)[1 \; + \; \frac{16}{\sqrt{2}} \, (\frac{G_F q^2}{4\pi\alpha}) \, (\frac{g_A g_V^s}{Q_s}) \, P] \tag{45}$$

Thus we conclude that in the ratio of Equation (44), all the hadronic dependence will cancel out for any decay channel. Then the result will be

$$A_{LR} = -\frac{12}{\sqrt{2}} \left(\frac{G_F q^2}{4\pi\alpha}\right) g_V^s \, P \qquad (46)$$

where g_V^s is the vector coupling of the Z to $s\bar{s}$ and we have used $g_A = \frac{1}{4}$ and $Q_s = -\frac{1}{3}$ defined in Appendix C. We have supposed Φ-dominance for all the channels F.

Equation (46) is valid for all decay channels and its value for $q^2 \simeq M_\Phi^2$ and $\sin^2\theta_W = 0.23$ is $1.94 \times 10^{-4} P$. So from the statistical point of view, it probably could be measured at DAΦNE by going to the dominant channels, that is, K^+K^-, $K_S K_L$ and $\rho\pi$, if a polarized beam of electrons is used.

Other observables can be defined for each particular channel. A Left-Right differential asymmetry (not integrated in θ) can be defined by

$$A_{LR}(\theta) = \frac{\frac{d\sigma}{d\Omega}(\theta, P = +1) - \frac{d\sigma}{d\Omega}(\theta, P = -1)}{\frac{d\sigma}{d\Omega}(\theta, P = +1) + \frac{d\sigma}{d\Omega}(\theta, P = -1)} \qquad (47)$$

From these observables we can recover Eq. (44) by integrating numerator and denominator separately. For the $\rho\pi$ channel, for example, we get

$$A_{LR}(\theta) = \frac{2Re[\frac{T_{1,1}(\Phi_Z)}{T_{1,1}(\Phi_\gamma)}](1 + \cos^2\theta) + 4Re[\frac{T_{1,1}(a_1^V) + T_{1,1}(\Phi - a_1)}{T_{1,1}(\Phi_\gamma)}]\cos\theta}{(1 + \cos^2\theta)} \qquad (48)$$

that obviously reproduces Eq. (44) and verifies the relation

$$A_{LR}(\theta = 0) = P_{z'}(\theta = 0) \qquad (49)$$

as can be checked from Eq. (14). This last relation is a direct consequence of angular momentum conservation and helicity conservation at the leptonic vertex. From this general relation we have a consistency check between Eq. (48) and Eq. (14).

Comparing Eqs. (48) and (14), we can see that the angular dependences of the differential left-right asymmetry for polarized beams, and the longitudinal polarization of the ρ for unpolarized beams are exchanged. In Eq. (14), the term with $\cos\theta$ is due to Parity violation in the leptonic vertex, that is, it comes from the decay of a polarized Φ, whereas the term with $(1 + \cos^2\theta)$ is due to Parity violation in Φ decay or interference with a_1-decay. However,

in the case of initial beam polarization, the term with parity violation in the leptonic vertex induces a left-right asymmetry even in the total cross section.

From Eq. (48), one can build a combined left-right forward-backward asymmetry as

$$A_{LR}^{FB} = \frac{\sigma_R(\cos\theta > 0) - \sigma_R(\cos\theta < 0) - \sigma_L(\cos\theta > 0) + \sigma_L(\cos\theta < 0)}{\sigma_R(\cos\theta > 0) + \sigma_R(\cos\theta < 0) + \sigma_L(\cos\theta > 0) + \sigma_L(\cos\theta < 0)} \quad (50)$$

to separate out the two terms in Eq. (48). Under the assumptions for the a_1-vertex form factors discussed in Section 5, we get $A_{LR}^{FB} \simeq 3.15 \times 10^{-6}$.

7   Conclusions

A general analysis of the possibilities of measuring $\gamma - Z$ interference at a Φ-factory has been worked out. For the case of unpolarized beams we have looked carefully to the K^+K^-, $K_L K_S$ and $\rho\pi$ channels. The first two channels do not present any distinctive signature of the interference. The $\rho\pi$ channel presents several signatures of the $\gamma - Z$ interference through parity violating observables, taking into account that the Z boson couples through the axial current to the a_1-meson that dominantly decays to $\rho\pi$. It is rather unfortunate the fact that the interference of Figures 1 and 2 only contributes to the ρ longitudinal polarization, a difficult observable to be measured. Nevertheless g_V^s enters in other asymmetries through ρ alignments, but the final values of these observables are rather small. C-odd asymmetries coming from the (V-V) (A-A) interference are of the order 10^{-5}, probably also out of DAΦNE performances, in addition other non-weak contribution has to be computed to give a definite prediction for $\langle\cos\theta\rangle$ and $\langle\cos\theta_1\cos\phi_1\rangle$. Potentially interesting two photon physics could also be present in these observables.

In the case of e^+e^- collision at $q^2 \simeq M_\Phi^2$ with longitudinally polarized electrons and unpolarized positrons, we have obtained that in every channel there is a left-right asymmetry of order 2×10^{-4}, free from hadronic uncertainties at leading order and sensitive to the vector coupling of the Z to the quark s. From the statistical point of view, this asymmetry seems to be reachable by DAΦNE operating with polarized electrons. We have also defined a combined left-right forward-backward asymmetry to extract

the (P-odd,T-even) $a_1 - \Phi$ interference. Its value is much smaller than the left-right asymmetry.

Acknowledgements

APPENDIX A

The ρ^{out} matrix for the ρ can be written, in the case of unpolarized beams, as

$$(\rho^{out})_{\sigma,\sigma'} = \sum_{\vec{\lambda}} f_{\sigma,\vec{\lambda}}(\theta,\phi)\, f^*_{\sigma',\vec{\lambda}}(\theta,\phi) = \sum_{\lambda} d^1_{\lambda,\sigma}(\theta) d^1_{\lambda,\sigma'}(\theta)\, T_{\sigma,\lambda} T^*_{\sigma',\lambda} \qquad \text{(A.1)}$$

In its center of mass frame or in any boosted frame along z', ρ^{out} can be written as

$$\frac{\rho^{out}}{Tr(\rho^{out})} = \frac{1}{2j+1} \sum_{L,M}^{2j} t^*_{L,M} T_{L,M} \qquad \text{(A.2)}$$

where the irreducible tensor operators are refered to the x' ,y' ,z' system defined by the helicity convention in Figure 5. Definition and normalization of $T_{L,M}$ follows the conventions in reference [5], the physical observables of the ρ will be given by

$$Tr(\rho^{out}) t_{L,M}(\theta) = Tr(\rho^{out} T_{L,M}) = \sum_{\sigma,\sigma'} (\rho^{out})_{\sigma,\sigma'} C(1L1|\sigma M \sigma') \qquad \text{(A.3)}$$

The multipole parameters $t_{L,M} = (-)^M t^*_{L,-M}$ define completely the ρ^{out} density matrix.

For completeness, we also give the ρ polarization in terms of the multi-polar parameters

$$P_{x'} = -(t_{1,1} - t_{1,-1}) = -2\ Re[t_{1,1}] \qquad \text{(A.4)}$$

$$P_{y'} = i(t_{1,1} + t_{1,-1}) = -2\ Im[t_{1,1}] \qquad \text{(A.5)}$$

$$P_{z'} = \sqrt{2}\ t_{1,0} \qquad \text{(A.6)}$$

19

APPENDIX B

In what follows, we shall define the form factors needed to performe our calculation. Also we shall give expressions of related processes where to measure these form factors.

The vector form factor is defined by

$$\langle \Phi(\vec{q}, \omega) \mid \bar{\psi}_s(0)\gamma_\mu\psi_s(0) \mid 0\rangle = F_V(q^2)\ \varepsilon^*(\omega, \vec{q})_\mu \tag{B.1}$$

it represents the coupling of the strange quark vector current to a Φ of momentum q and helicity ω, $\varepsilon^\mu(\omega, \vec{q})$ is the polarization four-vector of the Φ. With the one particle states normalized to $(2E)(2\pi)^3\delta^3(\vec{q}-\vec{q'})\delta_{\omega,\omega'}$, a straightforward calculation for the width of Φ going to e^-e^+ gives the result

$$\Gamma_{\Phi \to e^+e^-} = \frac{4\pi\alpha^2}{27}\frac{|F_V(M_\Phi^2)|^2}{M_\Phi^3} \tag{B.2}$$

The most general matrix element of a Φ with momentum q and helicity ω, going to a ρ with momentum k and helicity σ and a pion of momentum p is

$$\langle \rho(\vec{k}, \sigma)\ \pi(\vec{p}) \mid H \mid \Phi(\vec{q}, \omega)\rangle = i\Phi(q^2)\ \epsilon_{\mu\nu\alpha\beta}\ k^\mu\varepsilon(\omega, \vec{q})^\nu q^\alpha \xi^*(\sigma, \vec{k})^\beta \tag{B.3}$$

where $\xi(\sigma, \vec{k})^\beta$ is the polarization four-vector of the ρ. This result depends upon Lorentz invariance, linearity with the ρ and Φ wave functions, and parity conservation. We define $\Phi^{+,-,0}(q^2)$ corresponding to the three channels $\rho^+\pi^-$, $\rho^-\pi^+$ and $\rho^0\pi^0$. By using isospin we get

$$\Phi(q^2) = \Phi^+(q^2) = \Phi^-(q^2) = -\Phi^0(q^2) \tag{B.4}$$

From (B.3) we obtain

$$\Gamma(\Phi \to \rho^+\pi^-) = \frac{|\vec{k}|^3\ |\Phi(M_\Phi^2)|^2}{12\pi} \tag{B.5}$$

if we neglect the mass difference between the π^0 and the $\pi^\pm$.

The axial form factors are defined in the following way

$$\frac{1}{2}\langle a_1^0(\vec{q}, \omega) \mid \bar{\psi}_u(0)\gamma_\mu\gamma_5\psi_u(0) - \bar{\psi}_d(0)\gamma_\mu\gamma_5\psi_d(0) \mid 0\rangle = F_A(q^2)\ \varepsilon^*(\omega, \vec{q})_\mu \tag{B.6}$$

$$\langle a_1^{\pm}(\vec{q},\omega) \mid \frac{1}{\sqrt{2}} \bar{\psi}_{u,d}(0)\gamma_\mu\gamma_5\psi_{d,u}(0) \mid 0\rangle = F_A^{\pm}(q^2)\ \varepsilon^*(\omega,\vec{q})_\mu \qquad \text{(B.7)}$$

The notation is the same as in (B.1). Because the a_1 is isovector, we have the contribution of the isovector axial-vector current. From isospin we have

$$F_A(q^2) = F_A^+(q^2) = -F_A^-(q^2) \qquad \text{(B.8)}$$

By treating the a_1 in the narrow width approximation, one can extract [10] from $\tau^- \to \nu_\tau \pi\pi\pi$ an aproximate experimental data for $\tau^- \to \nu_\tau a_1^-$. For this process we get

$$\Gamma(\tau \to \nu_\tau a_1^-) = \frac{G_F^2}{8\pi}\ |V_{u,d}|^2\ |F_A^-(M_{a_1}^2)|^2\frac{M_\tau^3}{M_a^2}\ (1-\frac{M_a^2}{M_\tau^2})^2\ (1+2\frac{M_a^2}{M_\tau^2}) \quad \text{(B.9)}$$

Here , $V_{u,d}$ is the corresponding element of the Cabibbo-Kobayashi-Maskawa matrix, and the rest of the notation is self explanatory.

The most general matrix element of an a_1 with momentum q and helicity ω going to $\rho\pi$ is

$$\langle \rho^i(\vec{k},\sigma)\ \pi^j(\vec{p}) \mid H_S \mid a_1^k(\vec{q},\omega)\rangle = A_0^{i,j,k}(q^2)\ q^\mu\xi^*(\sigma,\vec{k})_\mu\ k^\nu\varepsilon(\omega,\vec{q})_\nu$$
$$+A_1^{i,j,k}(q^2)\ \{\frac{M_\rho^2 q^2 - (k\cdot q)^2}{(k\cdot q)}\ \varepsilon(\omega,\vec{q})_\alpha\xi^*(\sigma,\vec{k})^\alpha + q^\mu\xi^*(\sigma,\vec{k})_\mu\ k^\nu\varepsilon(\omega,\vec{q})_\nu)\}$$
$$\text{(B.10)}$$

Here we have two form factors: $A_1^{i,j,k}$ contributes to the amplitudes where the ρ is in the +1 or -1 helicity state, and $A_0^{i,j,k}$ to the 0 helicity state of the ρ. The general structure (B.10) depends upon the same asumptions we have used in (B.3). The indices i, j, k indicate the corresponding charges of each channel. From Isospin we have

$$A_\alpha^{i,j,k} = \sqrt{2}C(111|I_iI_jI_k)A_\alpha \qquad \text{(B.11)}$$

in such a way the a_1^0 does not decay to $\rho^0\pi^0$ and

$$A_\alpha = A_\alpha^{+,-,0} = -A_\alpha^{-,+,0} = A_\alpha^{0,-,-} = -A_\alpha^{-,0,-} \qquad \text{(B.12)}$$

21

We must point out that both (B.3) and (B.10) are valid for ρ and π both on shell, otherwise there would be other dependences with its invariant masses.

The width of the a_1 is given by

$$\Gamma_{a_1^i \to \rho^j \pi^k} = \frac{\lambda^{5/2}(M_a^2, M_\rho^2, M_\pi^2)}{768\pi M_a^5 M_\rho^2}\{|A_1^{i,j,k}(q^2)|^2 \frac{8M_\rho^2 M_a^2}{(M_a^2 + M_\rho^2 - M_\pi^2)^2} + |A_0^{i,j,k}(q^2)|^2\}$$

(B.13)

Separate information on A_0 and A_1 needs additional information about the a_1-decay, that could be extracted through a careful analysis of the $\tau \to \nu_\tau \pi \pi \pi$ decay [13]

APPENDIX C

In this section, we present the calculation of the reduced helicity amplitudes of the $e^+e^- \to \rho^+\pi^-$ process. The Kinematics in the C.M. frame of the e^+e^- system (or the Φ system) is defined by

$$l_-^\mu = (E, 0, 0, |\vec{l}|) \qquad\qquad q^\mu = (l_- + l_+)^\mu \qquad\qquad \text{(C.1)}$$

$$l_+^\mu = (E, 0, 0, -|\vec{l}|) \quad \xi^\mu(0, \vec{k}) = \tfrac{1}{M_\rho}(|\vec{k}|, k^0 \sin\theta, 0, k^0 \cos\theta)$$

$$k^\mu = (k^0, |\vec{k}|\sin\theta, 0, |\vec{k}|\cos\theta) \quad \xi^\mu(\pm 1, \vec{k}) = \mp\tfrac{1}{\sqrt{2}}(0, \cos\theta, \pm i, -\sin\theta)$$

The amplitudes we need correspond to the diagrams in Figures 1 to 4. Every vertex has been previously defined in Appendix B. The Φ and the a_1 propagators will be taken as pure Breit-Wigner distributions, although, more sophisticated versions can be taken if necessary. Relative phases have been imposed by the T properties of the currents, in such a way that relative imaginary pieces come essentially from the Breit-Wigner structure. The Feynman amplitudes corresponding to diagrams 1 to 3 are

$$M_{\sigma,\lambda_+,\lambda_-}^{\Phi\gamma}(\theta) = i\frac{4\pi\alpha}{q^2}Q_s F_V(q^2)\Phi(q^2)P_\Phi(q^2)V_\mu(\lambda_+,\lambda_-)\epsilon^{\mu\nu\alpha\beta}\xi_\nu^*(\sigma,\vec{k})k_\alpha q_\beta \tag{C.2}$$

$$M_{\sigma,\lambda_+,\lambda_-}^{\Phi z}(\theta) = i\frac{8G_F}{\sqrt{2}}g_V^s F_V(q^2)\Phi(q^2)P_\Phi(q^2)[g_V V^\mu(\lambda_+,\lambda_-) + g_A A^\mu(\lambda_+,\lambda_-)]$$
$$\epsilon^{\mu\nu\alpha\beta}\xi_\nu^*(\sigma,\vec{k})k_\alpha q_\beta \tag{C.3}$$

$$M_{\sigma,\lambda_+,\lambda_-}^{a_1}(\theta) = -\frac{8G_F}{\sqrt{2}}g_{3A}F_A(q^2)P_{a_1}(q^2)[g_V V^\mu(\lambda_+,\lambda_-) + g_A A^\mu(\lambda_+,\lambda_-)]$$
$$\{A_1(q^2)\frac{M_\rho^2 q^2 - (k\cdot q)}{(k\cdot q)}\xi_\mu^*(\sigma,\vec{k}) + [A_1(q^2) + A_0(q^2)](q\cdot\xi^*(\sigma,\vec{k}))k_\mu\}\tag{C.4}$$

The amplitude corresponding to diagram 4, $M_{\sigma,\lambda_+,\lambda_-}^{\Phi-a_1}$, can be obtained from $M_{\sigma,\lambda_+,\lambda_-}^{a_1}$ by taking $g_A = 0$, and performing the substitution

$$g_V \to -\frac{4\pi\alpha}{q^2}P_\Phi(q^2)|F_V(q^2)|^2 Q_s g_V^s \eta \tag{C.5}$$

In this expresions, $Q_s = -\frac{1}{3}$ is the s-quark charge, $g_V = -\frac{1}{4} + \sin^2 \theta_W$ and $g_A = \frac{1}{4}$ are the Z couplings to leptons, $g_{3A} = -\frac{1}{2}$ is the isovector axial-vector coupling to light quarks, and $g_V^s = -\frac{1}{4} + \frac{1}{3} \sin^2 \theta_W$ is the vector coupling of the Z to the s-quarks. Note that the precise normalization of the currents entering in the form factors is defined in (B.7). $P_\Phi(q^2)$ and $P_{a_1}(q^2)$ are the Φ and a_1 propagators respectively. We will take the usual Breit-Wigner structure

$$P(q^2) = \frac{1}{(q^2 - M^2) + iM\Gamma} \tag{C.6}$$

and the matrix element of the leptonic currents are given by

$$V^\mu(\lambda_-, \lambda_+) = \bar{v}(l_+, \lambda_+)\gamma^\mu u(l_-, \lambda_-) = 2E \,\delta_{-\lambda_+, \lambda_-}(0, \lambda_- - \lambda_+, i, 0)$$
$$A^\mu(\lambda_-, \lambda_+) = \bar{v}(l_+, \lambda_+)\gamma^\mu \gamma_5 u(l_-, \lambda_-) = 2E \,\delta_{-\lambda_+, \lambda_-}(0, 1, i(\lambda_- - \lambda_+), 0)$$
$$\tag{C.7}$$

It must be stressed that the weak hamiltonian entering in the amplitude $M_{\sigma, \lambda_+, \lambda_-}^{\Phi - a_1}$ is a pure non-leptonic one, so there can be additional contributions. Double Cabibbo suppressed charged current contributions are also present. From the analysis [14], the QCD corrections give rise to the factor $\eta \simeq 1.5$ in (C.5). The diagram in Figure 4 has been recently considered in ref [15], as "the parity violating piece of the weak decay $\Phi \to \rho\pi$" in the context of Chiral Perturbation Theory for vector mesons. We will not follow this calculation, because a_1-dominance has not been included, as the experimental data in $\tau \to \pi\pi\pi\nu_\tau$ [13] indicate, even at 1 GeV.

On the Φ-peak the (r.h.s.) of (C.5) can be written as

$$- i\, \frac{9\, \eta\, g_V^s}{\alpha}\, B.r.(\Phi \to e^+ e^-) \tag{C.8}$$

in such a way that for $\sin^2 \theta_W = 0.23$, it is 3.3η times bigger than the (l.h.s.) in (C.5).

Finally the normalization in Equations (C.2), (C.3) and (C.4) is such that

$$\sigma(e^+ e^- \to \rho\, \pi) = \frac{1}{8q^2} \int \frac{d^3k}{2k^0} \frac{d^3p}{2p^0} \frac{1}{2\pi^2} \sum_{\sigma, \lambda_+, \lambda_-} |M_{\sigma, \lambda_+, \lambda_-}(\Phi + a_1)|^2 \delta^{(4)}(q - k - p) \tag{C.9}$$

24

From the Φ-diagram we get

$$\sigma(e^+e^- \to \rho\,\pi)|_{q^2 \simeq M_\Phi^2} \simeq \frac{12\pi\Gamma(\Phi \to e^+e^-)\Gamma(\Phi \to \rho^+\pi^-)}{(q^2 - M_\Phi^2)^2 + M_\Phi^2\Gamma_\Phi^2} \qquad (C.10)$$

where the equality holds in the range where the q^2-dependence of $F_V(q^2)$ and $\Phi(q^2)$ can be neglected, a very good approximation arround the Φ-peak.

A lengthy but straightforward calculation has allowed to check the relation

$$M_{\sigma,\lambda_+,\lambda_-}(\theta) = K f_{\sigma,\vec{\lambda}}(\theta) \qquad (C.11)$$

for both Φ and a_1 contributions. K is a q^2-dependent constant that takes care of the different normalizations in Equation (C.9) and (7) and (6).

Finally we get the following results

$$KT_{1,1}(\Phi_\gamma) = -4\pi \sqrt{2}\alpha Q_s \,|\vec{k}| \, F_V(q^2)\Phi(q^2)P_\Phi(q^2) \qquad (C.12)$$

$$KT_{1,1}(\Phi_Z) = -8 \, G_F q^2 \, g_V^s \, g_A \, |\vec{k}| \, F_V(q^2)\Phi(q^2)P_\Phi(q^2) \qquad (C.13)$$

$$KT_{0,1}(a_1^V) = -8 \, G_F q^2 \, g_V g_{3A} \, \frac{|\vec{k}|^2}{M_\rho} \, F_A(q^2) \, A_0(q^2)P_{a_1}(q^2) \qquad (C.14)$$

$$KT_{1,1}(a_1^V) = 8 \, G_F q^2 \, g_V g_{3A} \, \frac{|\vec{k}|^2}{k^0} \, F_A(q^2)A_1(q^2)P_{a_1}(q^2) \qquad (C.15)$$

$$KT_{0,1}(a_1^A) = -8 \, G_F q^2 \, g_A g_{3A} \, \frac{|\vec{k}|^2}{M_\rho} \, F_A(q^2) \, A_0(q^2)P_{a_1}(q^2) \qquad (C.16)$$

$$KT_{1,1}(a_1^A) = 8 \, G_F q^2 \, g_A g_{3A} \, \frac{|\vec{k}|^2}{k^0} \, F_A(q^2)A_1(q^2)P_{a_1}(q^2) \qquad (C.17)$$

$KT_{0,1}(\Phi - a_1)$ and $KT_{1,1}(\Phi - a_1)$ can be obtained from (C.14) and (C.15) respectively just performing the substitution (C.5).

The following relations have been checked out explicitly

$$T_{1,1}(\Phi_\gamma) = T_{1,-1}(\Phi_\gamma) = -T_{-1,-1}(\Phi_\gamma) = -T_{-1,1}(\Phi_\gamma) \qquad \text{(C.18)}$$

$$T_{1,1}(\Phi_Z) = -T_{1,-1}(\Phi_Z) = T_{-1,-1}(\Phi_Z) = -T_{-1,1}(\Phi_Z) \qquad \text{(C.19)}$$

$$
\begin{aligned}
T_{0,1}(a_1^V, \Phi - a_1) &= T_{0,-1}(a_1^V, \Phi - a_1) && \text{(C.20)}\\
T_{1,1}(a_1^V, \Phi - a_1) = T_{1,-1}(a_1^V, \Phi - a_1) &= T_{-1,1}(a_1^V, \Phi - a_1) = T_{-1,-1}(a_1^V, \Phi - a_1)
\end{aligned}
$$

$$
\begin{aligned}
T_{0,1}(a_1^A) &= -T_{0,-1}(a_1^A) && \text{(C.21)}\\
T_{1,1}(a_1^A) = -T_{1,-1}(a_1^A) &= T_{-1,1}(a_1^A) = -T_{-1,-1}(a_1^A)
\end{aligned}
$$

These are equivalent to Equations (4) and (5).

References

[1] G. Vignola, *Proceeding of the Worshop on Physics and Detectors for DAΦNE*, ed G. Pancheri, (INFN, Frascati 1991), p. 11.
A. N. Skrinsky,*Proceeding of the Worshop on Physics and Detectors for DAΦNE*, ed G. Pancheri, (INFN, Frascati 1991), p. 67.

[2] *The DAΦNE Physics Handbook*, eds L. Maiani, G. Pancheri and N.Paver, (INFN, Frascati 1992).
The Second DAΦNE Physics Handbook, eds L. Maiani, G. Pancheri and N.Paver, (INFN, Frascati 1995).

[3] Particle Data Group, M. Aguilar-Benitez *et al.*, *Phys. Rev.* **D50**, 1173 (1994).

[4] Private comunication by G. Vignola.

[5] A.D. Martin, T.D. Spearman, "Elementary Particle Theory", North-Holland, Amsterdam 1970.

[6] L.D. Landau, *Dokl. Akad. Nawk.*, USSR **60**, 207 (1948). Sumary in English in *Phys. Abstracts* **A52**, 125 (1949).
C.N. Yang, *Phys. Rev.* **77**, 242 (1950).

[7] J.H. Kühn, J. Kaplan and E.G.O. Safiani, *Nucl. Phys.* **B157**, 125 (1979)

[8] J. Prades, *Z. Phys* **C63**, 491 (1994)

[9] Work in progress.

[10] W.T. Ford, *Nucl. Phys. B (Proc. Suppl.)* **40**, 191 (1995).
J.H. Kühn and A. Santamaria, *Z. Phys.* **C48** , 445 (1990).

[11] M. Wingate, T. DeGrand, S. Collins, and U. Heller, *Phys. Rev. Lett.* **74**, 4596 (1995).

[12] N. Isgur, C. Morningstar and C. Reader, *Phys. Rev.* **D39**, 1357 (1989).

[13] ARGUS Collaboration, H. Albretch *et al.*, *Z. Phys.* **C58**, 61 (1993).

[14] J. Dai, M.J. Savage, J. Liu and R. Springer, *Phys. Lett.* **B271**, 403 (1991).

[15] E. Jenkins, A. Manohar, and M. Wise, *Phys. Rev. Lett.* **75**, 2272 (1995).

Table Captions

Table I: Dominant Φ decay channels.

Table I

$\Phi(1020)$	$I^G(J^{PC}) = 0^-(1^{--})$
Mass $M_\Phi = 1019.413 \pm 0.008\ MeV$	
Width $\Gamma = 4.43 \pm 0.06\ MeV$	
Decay modes	Fraction Γ_i/Γ
K^+K^-	$(49.1 \pm 0.9)\%$
$K^0_L K^0_S$	$(34.3 \pm 0.7)\%$
$\rho\,\pi$	$(12.9 \pm 0.7)\%$
$\pi^+\pi^-\pi^0$	$(2.5 \pm 0.9)\%$
$\eta\,\gamma$	$(1.28 \pm 0.06)\%$
$\pi^0\,\gamma$	$(1.31 \pm 0.13) \times 10^{-3}$
$e^+\,e^-$	$(3.09 \pm 0.07) \times 10^{-4}$
$\mu^+\,\mu^-$	$(2.48 \pm 0.34) \times 10^{-4}$

Figure Captions

Figure 1: Dominat diagram for Φ production at a Φ-factory.

Figure 2: Z-mediated production of Φ. V (A) means a vector (axial) coupling.

Figure 3: Pure a_1 resonant contribution, mediated by Z.

Figure 4: Weak decay of Φ through a_1.

Figure 5: Reference system. (x, y, z) define the axes in the C.M. of the e^+e^- system. (x', y', z') are the corresponding axes in the ρ C.M. frame of reference.

Figure 6: Real and Imaginary part of $G(\epsilon)$, defined in Equation (33). The Breit-Wigner structure of the Φ has been included.
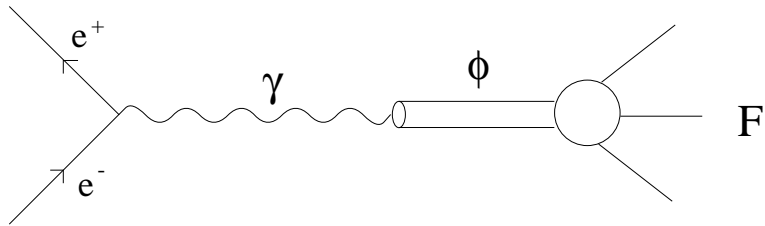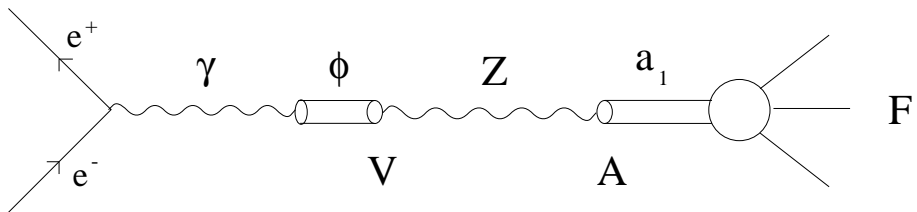
Fig 1.

Fig 2.

Fig 3.

Fig 4.

Fig 5.

Fig 6.